Double Shadowing the Rician Fading Model

Published in:
IEEE Wireless Communications Letters

Document Version:
Peer reviewed version

Double Shadowing the Rician Fading Model

Nidhi Bhargav, *Student Member, IEEE*, Carlos Rafael Nogueira da Silva, Simon L. Cotton, *Senior Member, IEEE*,
Paschalis C. Sofotasios, *Senior Member, IEEE* and Michel Daoud Yacoub, *Member, IEEE*

Abstract—In this letter, we consider a Rician fading envelope which is impacted by dual shadowing processes. We conveniently refer to this as the double shadowed Rician fading model which can appear in two different formats, each underpinned by a different physical signal reception model. The first format assumes a Rician envelope where the dominant component is fluctuated by a Nakagami-m random variable (RV) which is preceded (or succeeded) by a secondary round of shadowing brought about by an inverse Nakagami-m RV. The second format considers that the dominant component and scattered waves of a Rician envelope are perturbed by two different shadowing processes. In particular, the dominant component experiences variations characterized by the product of a Nakagami-m and an inverse Nakagami-m RV, whereas the scattered waves are subject to fluctuations influenced by an inverse Nakagami-m RV. Using the relationship between the shadowing properties of the two formats, we develop unified closed-form and analytical expressions for their probability density function, cumulative distribution function, moment-generating function and moments. All of the expressions are validated through Monte Carlo simulations and reduction to a number of special cases.

Index Terms—Composite fading, fading channels, inverse Nakagaim-m distribution, shadowed Rician model.

I. INTRODUCTION

Several statistical distributions have been proposed to characterize fading in wireless channels [1]. Shadowing is commonly modeled using the lognormal distribution [1] whilst multipath fading is described by the Rayleigh, Rice, Nakagami-m, and more recently κ-μ and η-μ [2] distributions. Nevertheless, these models are unable to account for fluctuations of the line-of-sight (LOS) or scattered signal contributions brought about by shadowing. Hence, several composite fading models have been proposed which address these shortcomings. The shadowing in these is LOS if the dominant component of the envelope is shadowed, and multiplicative when the total power of the dominant (if present) and scattered components are shadowed. A number of multiplicative shadow fading models were proposed in [3]–[6]. These include the Nakagami-m/gamma [3], κ-μ/gamma [4], η-μ/gamma [5], κ-μ/inverse gamma and η-μ/ inverse gamma models [6].

N. Bhargav, and S. L. Cotton are with the Institute of Electronics, Communications and Information Technology, The Queen's University of Belfast, BT3 9DT, UK. Email: {nbhargav01, simon.cotton}@qub.ac.uk.

C. R. N da Silva and M. D. Yacoub are with the Wireless Technology Laboratory, School of Electrical and Computer Engineering, University of Campinas, 13083-970, Brazil. E-mail: {carlosrn, michel}@decom.fee.unicamp.br.

P. C. Sofotasios is with the Department of Electrical and Computer Engineering, Khalifa University of Science and Technology, PO Box 127788, UAE, and the Department of Electronics and Communications Engineering, Tampere University of Technology, FI-33720, Finland. E-mail: p.sofotasios@ieee.org.

Here, we focus on the shadowed Rician model [7] which considers a Rician envelope in which the LOS is perturbed by shadowing shaped by a Nakagami-m random variable (RV). This model has good analytical properties [8] and provides an excellent fit to data obtained from land mobile satellite and underwater acoustic channels [7], [9]. Motivated by this, we introduce the double shadowed Rician fading model which can appear in two formats. The first format considers a Rician signal in which the LOS undergoes variations influenced by a Nakagami-m RV. It also assumes that the root mean square (rms) power of the dominant component and scattered waves undergo a secondary round of shadowing shaped by an inverse Nakagami-m RV. The second format assumes that the dominant component of a Rician envelope undergoes fluctuations characterized by the product of a Nakagami-m and an inverse Nakagami-m RV, whilst the scattered waves are fluctuated by an inverse Nakagami-m RV. The PDF, cumulative distribution function (CDF), moment generating function (MGF) and moments are derived which are coincidentally identical for both formats, differing only in the interpretation of the underlying physical phenomena. These results are then used to obtain their amount of fading (AF) and outage probability (OP).

II. THE PHYSICAL MODEL

The PDF of the shadowed Rician fading model [7] is

$$f_X(x) = \left(\frac{2\sigma^2 m_d}{2\sigma^2 m_d + d^2}\right)^{m_d} \frac{x}{\sigma^2} e^{\frac{-x^2}{2\sigma^2}} {}_1F_1\left(m_d; 1; \frac{d^2 x^2}{2\sigma^2(2\sigma^2 m_d + d^2)}\right) \tag{1}$$

where, ${}_1F_1(\cdot; \cdot; \cdot)$ denotes the confluent hypergeometric function [10, 9.210.1], m_d denotes the shape parameter of the Nakagami-m RV, $2\sigma^2$ is the average power of the scattered component, and d^2 is the average power of the LOS component. Here, $k = \frac{d^2}{2\sigma^2}$ is the Rician k parameter, and $\hat{x} = \sqrt{\mathbb{E}[X^2]} = \sqrt{2\sigma^2 + d^2}$ represents the rms power of X, where $\mathbb{E}[\cdot]$ is the expectation operator. We rewrite (1) as

$$f_X(x) = \frac{m_d^{m_d} 2x(1+k)}{(k+m_d)^{m_d} \hat{x}^2} e^{-(1+k)\frac{x^2}{\hat{x}^2}} {}_1F_1\left(m_d; 1; \frac{k(1+k)x^2}{\hat{x}^2(m_d+k)}\right). \tag{2}$$

The first format of the double shadowed Rician model assumes a Rician fading channel which undergoes LOS shadowing followed by a secondary round of composite shadowing or vice versa. Physically, this may arise when the signal power delivered through the direct path between the transmitter and receiver is subject to varying levels of shadowing, whilst further shadowing of the received power (combined scattered multipath and LOS) is due to obstacles moving in the vicinity of either the transmitter or receiver. Its signal envelope, R, is

$$R^2 = A^2\left[(I + \xi\mu_x)^2 + (Q + \xi\mu_y)^2\right] \tag{3}$$

where I and Q are mutually independent Gaussian random processes with mean $\mathbb{E}[I] = \mathbb{E}[Q] = 0$ and variance $\mathbb{E}[I^2] = \mathbb{E}[Q^2] = \sigma^2$, μ_x and μ_y are the mean values of the in-phase and the quadrature phase components, respectively. In (3), ξ is a Nakagami-m RV with shape parameter m_d where $\mathbb{E}[\xi^2] = 1$, and A is an inverse Nakagami-m RV with shape parameter m_s, where $\mathbb{E}[A^2] = 1$, whose PDF is given by

$$f_A(\alpha) = \frac{2(m_s-1)^{m_s}}{\Gamma(m_s)\,\alpha^{2m_s+1}}\,\mathrm{e}^{-\frac{(m_s-1)}{\alpha^2}}. \tag{4}$$

Here, $\Gamma(\cdot)$ represents the Gamma function [10, 8.310.1].

The second format of the double shadowed Rician model assumes a Rician faded signal in which the dominant component and scattered waves are subject to two different shadowing processes. More precisely, the dominant component experiences variations characterized by the product of a Nakagami-m and an inverse Nakagami-m RV, whilst the scattered waves are subject to fluctuations influenced by an inverse Nakagami-m RV. Its signal envelope, R, is

$$R^2 = \left[(AI + B\mu_x)^2 + (AQ + B\mu_y)^2\right] \tag{5}$$

where $B = A\xi$, A and ξ are as defined above. It is worth highlighting that as shown in [11], B^2 follows a Fisher-Snedecor $\mathcal{F}$ distribution [11]. Now, substituting for B in (5), we obtain (3). Note that although (3) and (5) are mathematically identical, their physical meanings differ as explained above.

III. STATISTICAL CHARACTERISTICS

Exploiting the mathematical relationship above and selecting (3) as our starting point, the distribution of the received signal envelope, R, in a double shadowed Rician channel can be obtained by determining the conditional probability

$$f_R(r) = \int_0^\infty f_{R|A}(r|\alpha) f_A(\alpha)\,d\alpha; \tag{6}$$

$$f_{R|A}(r|\alpha) = \frac{2r(1+k)\,\mathrm{e}^{-(1+k)\frac{r^2}{\alpha^2\hat{r}^2}}\,{}_1F_1\!\left(m_d;1;\frac{k(1+k)r^2}{\alpha^2\hat{r}^2(m_d+k)}\right)}{m_d^{-m_d}(m_d+k)^{m_d}\alpha^2\hat{r}^2}. \tag{7}$$

Theorem 1. *For k, m_d, $\hat{r}^2$, $r \in \mathbb{R}^+$ and $m_s > 1$ the PDF of the double shadowed Rician fading model can be written as*

$$f_R(r) = \frac{2r\hat{r}^{2m_s}m_s(m_s-1)^{m_s}(1+k)}{(r^2(1+k)+(m_s-1)\hat{r}^2)^{m_s+1}}\left(\frac{m_d}{m_d+k}\right)^{m_d}$$
$$\times\, {}_2F_1\!\left(m_d, m_s+1; 1; \frac{k(1+k)r^2}{(m_d+k)(r^2(1+k)+(m_s-1)\hat{r}^2)}\right) \tag{8}$$

where ${}_2F_1(\cdot,\cdot;\cdot;\cdot)$ is the Gauss hypergeometric function [10].

Proof: See Appendix -A. ∎

Letting γ represent the instantaneous signal-to-noise-ratio (SNR) of the double shadowed Rician fading model, the PDF of its instantaneous SNR, $f_\gamma(\gamma)$, is obtained from the envelope PDF in (8) via a transformation of variables $\left(r = \sqrt{\gamma\,\hat{r}^2/\bar{\gamma}}\right)$,

$$f_\gamma(\gamma) = \frac{\bar{\gamma}^{m_s}m_s(m_s-1)^{m_s}(1+k)}{(\gamma(1+k)+(m_s-1)\bar{\gamma})^{m_s+1}}\left(\frac{m_d}{m_d+k}\right)^{m_d}$$
$$\times\, {}_2F_1\!\left(m_d, m_s+1; 1; \frac{k(1+k)\gamma}{(m_d+k)(\gamma(1+k)+(m_s-1)\bar{\gamma})}\right) \tag{9}$$

where $\bar{\gamma} = \mathbb{E}[\gamma]$ denotes the corresponding average SNR.

Lemma 1. *For k, m_d, $\bar{\gamma}$, $\gamma \in \mathbb{R}^+$, and $m_s > 1$ the CDF of the double shadowed Rician fading model, $F_\gamma(\gamma)$, can be obtained such that $F_\gamma(\gamma) = \int_0^\gamma f_\gamma(t)\,dt$, as*

$$F_\gamma(\gamma) = \sum_{i=0}^\infty \left(\frac{m_d}{m_d+k}\right)^{m_d}\left(\frac{k}{m_d+k}\right)^i \frac{(m_d)_i\,(i+1)_{m_s}}{\Gamma(m_s)\,\Gamma(i+2)}$$
$$\times\left(\frac{\gamma(1+k)}{(m_s-1)\bar{\gamma}}\right)^{i+1}\,{}_2F_1\!\left(i+1, i+m_s+1; i+2; -\frac{\gamma(1+k)}{(m_s-1)\bar{\gamma}}\right). \tag{10}$$

where $(x')_{n'} = \frac{\Gamma(x'+n')}{\Gamma(x')}$ denotes the Pochhammer symbol [10]. When $(m_s-1)\bar{\gamma} > \gamma(1+k)$,

$$F_\gamma(\gamma) = \frac{m_d^{m_d}m_s\gamma(1+k)}{(m_d+k)^{m_d}(m_s-1)\bar{\gamma}}$$
$$\times\, F_{1,1,0}^{2,1,0}\!\left(\begin{matrix} m_s+1, 1; & m_d; & -; \\ 2; & 1; & -; \end{matrix}\ \frac{k(1+k)\gamma}{(m_d+k)\bar{\gamma}(m_s-1)}, \frac{-(1+k)\gamma}{\bar{\gamma}(m_s-1)}\right) \tag{11}$$

where $F_{\cdot,\cdot,\cdot}^{\cdot,\cdot,\cdot}\!\left(\begin{smallmatrix} \cdot,\cdot; & \cdot; & \cdot; \\ \cdot; & \cdot; & \cdot; \end{smallmatrix}\ \cdot,\cdot\right)$ denotes the Kampé de Fériet function [12]. On the contrary, when $(m_s-1)\bar{\gamma} < \gamma(1+k)$,

$$F_\gamma(\gamma) = \frac{m_d^{m_d}}{(m_d+k)^{m_d}}\left[F_{0,1,1}^{1,1,1}\!\left(\begin{matrix} 1; m_d; & 0; \\ -; & 1; & 1-m_s; \end{matrix}\ \frac{k}{m_d+k}, \frac{-(m_s-1)\bar{\gamma}}{\gamma(1+k)}\right)\right.$$
$$\left. -\,\zeta'\,F_{0,1,1}^{1,1,1}\!\left(\begin{matrix} m_s+1; m_d; & m_s; \\ -; & 1; & 1+m_s; \end{matrix}\ \frac{k}{m_d+k}, \frac{-(m_s-1)\bar{\gamma}}{\gamma(1+k)}\right)\right] \tag{12}$$

where $\zeta' = \frac{((m_s-1)\bar{\gamma})^{m_s}\Gamma(m_s+1)}{m_s(\gamma(1+k))^{m_s}\Gamma(m_s)}$

Proof: See Appendix -A. ∎

Lemma 2. *For k, m_d, $\bar{\gamma}$, $\gamma \in \mathbb{R}^+$, and $m_s > 1$ the MGF of the double shadowed Rician fading model, $M_\gamma(s)$, can be obtained such that $M_\gamma(s) \triangleq \mathbb{E}[\mathrm{e}^{-s\gamma}] = \int_0^\infty \mathrm{e}^{-s\gamma}f_\gamma(\gamma)\,d\gamma$,*

$$M_\gamma(s) = \left(\frac{m_d}{m_d+k}\right)^{m_d}\left[\psi_1\!\left(1, m_d, 1, 1-m_s; \frac{k}{m_d+k}, \zeta\right)\right.$$
$$\left. +\,\frac{\zeta^{m_s}\Gamma(-m_s)}{B(m_s,1)}\psi_1\!\left(1+m_s, m_d, 1, 1+m_s; \frac{k}{m_d+k}, \zeta\right)\right] \tag{13}$$

where $\zeta = \frac{\bar{\gamma}(m_s-1)s}{1+k}$ and $\psi_1(\cdot,\cdot,\cdot,\cdot;\cdot,\cdot)$ is the Humbert ψ_1 function [13].

Proof: See Appendix -B. ∎

Lemma 3. *For k, m_d, $\bar{\gamma}$, $\gamma \in \mathbb{R}^+$, and $m_s > 1$ the n-th order moment of the double shadowed Rician fading model, $\mathbb{E}[\gamma^n]$, can be obtained such that $\mathbb{E}[\gamma^n] \triangleq \int_0^\infty \gamma^n f_\gamma(\gamma)\,d\gamma$, as*

$$\mathbb{E}[\gamma^n] = \frac{\Gamma(m_s-n)\,\Gamma(1+n)\,{}_2F_1\!\left(m_d, n+1; 1; \frac{k}{m_d+k}\right)}{m_d^{-m_d}(m_d+k)^{m_d}\Gamma(m_s)(1+k)^n[(m_s-1)\bar{\gamma}]^{-n}}. \tag{14}$$

Proof: See Appendix -B. ∎

IV. PERFORMANCE ANALYSIS

A. Amount of Fading

Corollary 1. *For $k \in \mathbb{R}^+$, $m_s > 2$, the AF of the double shadowed Rician fading model is obtained such that* $\mathrm{AF} \triangleq \frac{\mathbb{V}[\gamma]}{\mathbb{E}[\gamma]^2} = \frac{\mathbb{E}[\gamma^2]}{\mathbb{E}[\gamma]^2} - 1$, *where $\mathbb{V}(\cdot)$ denotes the variance operator,*

$$\mathrm{AF} = \frac{m_d m_s (1 + 2k) + (m_d + m_s - 1) k^2}{m_d (m_s - 2)(1 + k)}. \quad (15)$$

Proof: See Appendix -B. ∎

B. Outage Probability

Corollary 2. *For k, m_d, $\bar{\gamma} \in \mathbb{R}^+$ and $m_s > 1$ the OP of the double shadowed Rician fading model, can be obtained such that $P_{\mathrm{OP}}(\gamma_{\mathrm{th}}) \triangleq P[0 \leq \gamma \leq \gamma_{\mathrm{th}}] = F_\gamma(\gamma_{\mathrm{th}})$, as*

$$P_{\mathrm{OP}}(\gamma_{\mathrm{th}}) = \sum_{i=0}^{\infty} \left(\frac{m_d}{m_d + k} \right)^{m_d} \left(\frac{k}{m_d + k} \right)^i \frac{(m_d)_i (i+1)_{m_s}}{\Gamma(m_s) \Gamma(i+2)}$$

$$\times \left(\frac{\gamma_{\mathrm{th}}(1+k)}{(m_s - 1)\bar{\gamma}} \right)^{i+1} {}_2F_1\left(i+1, i+m_s+1; i+2; -\frac{\gamma_{\mathrm{th}}(1+k)}{(m_s - 1)\bar{\gamma}}\right) \quad (16)$$

where γ_{th} is the threshold SNR.

Proposition 1. *For $(m_s - 1)\bar{\gamma}(m_d + k) > \gamma_{\mathrm{th}}k(1 + k)$, the truncation error, $\mathcal{T}$, for the infinite series in (16) is given as*

$$\mathcal{T} \leq {}_2F_1\left(T_0+1, T_0+m_s+1; T_0+2; -\frac{\gamma_{\mathrm{th}}(1+k)}{(m_s-1)\bar{\gamma}}\right) \frac{\gamma_{\mathrm{th}}(1+k)}{(m_s-1)\bar{\gamma}}$$

$$\times m_s \ {}_2F_1\left(m_d, 1+m_s; 2; \frac{\gamma_{\mathrm{th}}k(1+k)}{(m_s-1)\bar{\gamma}(m_d+k)}\right). \quad (17)$$

Proof: See Appendix -C. ∎

V. SPECIAL CASES AND NUMERICAL RESULTS

The results presented here encompass the statistics of the shadowed Rician, shadowed Rayleigh, Nakagami-q, Rician and Rayleigh fading models. For example, letting $m_s \to \infty$ in (8) we obtain the PDF of the shadowed Rician model, and allowing $m_d \to 0$ in (8) we obtain the PDF of the shadowed Rayleigh model. Allowing $m_s \to \infty$ and $m_d = 0.5$ in (8) we obtain the PDF of the Nakagami-q (Hoyt) model, while letting
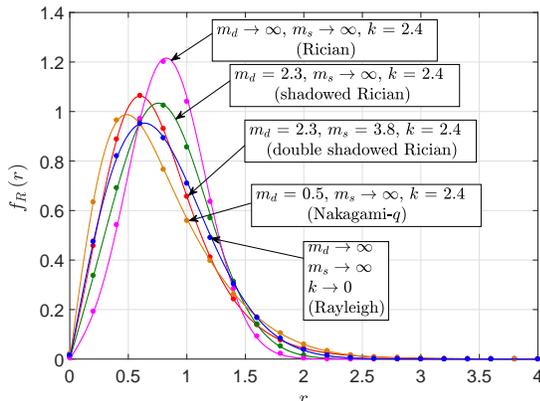

Fig. 1. Double shadowed Rician PDF alongside special cases. Lines represent analytical results, and circle markers represent simulation results ($\hat{r} = 0.9$).
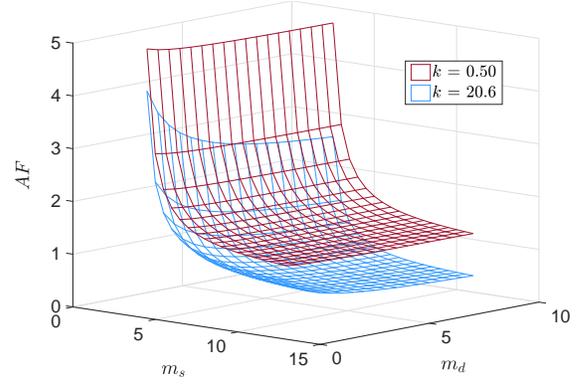

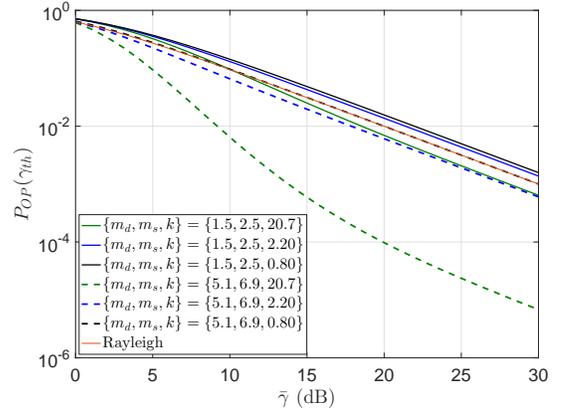Fig. 2. The AF in double shadowed Rician fading channels for a range of m_s and m_d when k = 0.5 and 20.6.

Fig. 3. OP versus $\bar{\gamma}$ for different values of m_d, m_s and k. Here $\gamma_{\mathrm{th}} = 0$ dB.

$m_s \to \infty$ and $m_d \to \infty$ in (8), the Rician PDF is obtained, followed by the Rayleigh fading model when $k \to 0$. Fig. 1 shows these special cases alongside Monte-Carlo simulations.

To provide some insights into the effect of shadowing upon the dominant and scattered multipath signal in double shadowed Rician fading channels, Fig. 2 shows the calculated AF for different values of m_d and m_s. Choosing the first format of the double shadowed Rician model, it is observed from Fig. 2 that the greatest AF occurs for severe shadowing of the multiplicative parameter (low m_s), when compared to the shadowing of the LOS component (m_d). For instance, the AF observed when $\{m_d, m_s, k\} = \{3.5, 2.5, 20.6\}$ is 3.05, which is greater compared to the AF observed when $\{m_d, m_s, k\} = \{2.5, 3.5, 20.6\}$, which is 1.42. From Fig. 3 we observe that the OP increases for severe shadowing of the LOS component (low m_d) and multiplicative parameter (low m_s), and low values of the Rician k parameter. Moreover the rate at which the OP decreases is faster as m_d, m_s and k parameters grow large.

VI. CONCLUSION

The double shadowed Rician fading model has been proposed in conjunction with two underlying signal models. It was shown that although the two formats have different physical meanings, mathematically they are identical. Consequently, fundamental statistics such as the PDF, CDF, MGF, and mo-

ments were obtained, while important performance measures such as the AF, and OP were also derived.

APPENDIX

A. Proof of (8), (10), (11) and (12)

The PDF of the double shadowed Rician model shown in (8) is obtained by first substituting (4) and (7) in (6), followed by solving the resultant integral using [10, eq. 7.621.4].

Replacing the Gauss hypergeometric function with [14, 07.23.02.0001.01] in (9), substituting the resultant expression in $F_\gamma(\gamma) = \int_0^\gamma f_\gamma(t)\,dt$, and solving the integral using [10, eq. 3.194.5] we obtain the CDF shown in (10). Now, substituting the Gauss hypergeometric function with [14, 07.23.02.0001.01] (for $(m_s-1)\bar{\gamma} > \gamma(1+k)$) in (10), using the Pochhammer symbol identities, and finally using the definition of Kampé de Feriét function [12], we obtain (11). On the contrary, substituting the Gauss hypergeometric function in (10) with [14, 07.23.02.0004.01] (for $(m_s-1)\bar{\gamma} < \gamma(1+k)$), using the Pochhammer symbol identities, and finally using the definition of Kampé de Feriét function, we obtain (12).

B. Proof of (13), (14) and (15)

Substituting (9) in $M_\gamma(s) = \int_0^\infty e^{-s\gamma} f_\gamma(\gamma)\,d\gamma$, followed by replacing the Gauss hypergeometric function with [14, 07.23.02.0001.01], we obtain an integral similar to [10, eq. 3.383.5]. Now substituting for the generalized Laguerre polynomial [10] given by $L_n^m(x) = \frac{\Gamma(m+n+1)}{\Gamma(m+1)\Gamma(n+1)} {}_1F_1(-n; m+1; x)$ and simplifying, we obtain

$$M_\gamma(s) = \sum_{i=0}^\infty \left(\frac{m_d}{m_d+k}\right)^{m_d} \left(\frac{k}{m_d+k}\right)^i \frac{(m_d)_i\,(i+1)_{m_s}}{\Gamma(m_s)\,i!}$$
$$\left[B(m_s, i+1)\,{}_1F_1\!\left(i+1; 1-m_s; \frac{\bar{\gamma}(m_s-1)s}{1+k}\right) + \left(\frac{\bar{\gamma}(m_s-1)s}{1+k}\right)^{m_s}\right.$$
$$\left.\Gamma(-m_s)\,{}_1F_1\left(i+m_s+1; 1+m_s; \frac{\bar{\gamma}(m_s-1)s}{1+k}\right)\right]. \quad (18)$$

By substituting the Kummer confluent hypergeometric function with [14, 07.20.02.0001.01] in (18), using the Pochhammer symbol identities, and finally using the definition of the Humbert ψ_1 function [13], we obtain (13).

The n-th order moment is obtained by first substituting [14, 07.23.02.0001.01] in (9), then substituting the resultant expression in $\mathbb{E}[\gamma^n] = \int_0^\infty \gamma^n f_\gamma(\gamma)\,d\gamma$ to obtain an integral identical to [10, eq. 3.194.3]. Now, using the identity [14, 07.23.02.0001.01] and simplifying, we obtain (14).

Substituting $n = 1$ and 2 into (14), we obtain the first and second moments of the double shadowed Rician model. Utilizing these in the AF formulation (see corollary 1), followed by using [14, 07.23.02.0001.01] and finally simplifying the resultant expression, we obtain the AF shown in (15).

C. Proof of (17) - Truncation Error

$\mathcal{T}$ for the series in (16) if $T_0 - 1$ terms are used, is

$$\mathcal{T} = \sum_{i=T_0}^\infty \left(\frac{k}{m_d+k}\right)^i \frac{(m_d)_i\,(i+1)_{m_s}}{\Gamma(i+2)\Gamma(m_s)} \left(\frac{\gamma_{\text{th}}(1+k)}{(m_s-1)\bar{\gamma}}\right)^{i+1}$$
$$\times\, {}_2F_1\left(i+1, i+m_s+1; i+2; -\frac{\gamma_{\text{th}}(1+k)}{(m_s-1)\bar{\gamma}}\right). \quad (19)$$

Since the Gauss hypergeometric function in (19) is monotonically decreasing with respect to i, $\mathcal{T}$ can be bounded as

$$\mathcal{T} \leq {}_2F_1\left(T_0+1, T_0+m_s+1; T_0+2; -\frac{\gamma_{\text{th}}(1+k)}{(m_s-1)\bar{\gamma}}\right)$$
$$\times \sum_{i=T_0}^\infty \left(\frac{k}{m_d+k}\right)^i \frac{(m_d)_i\,(i+1)_{m_s}}{\Gamma(i+2)\Gamma(m_s)} \left(\frac{\gamma_{\text{th}}(1+k)}{(m_s-1)\bar{\gamma}}\right)^{i+1}. \quad (20)$$

Since we add up strictly positive terms, we have

$$\sum_{i=T_0}^\infty \left(\frac{k}{m_d+k}\right)^i \frac{(m_d)_i\,(i+1)_{m_s}}{\Gamma(i+2)\Gamma(m_s)} \left(\frac{\gamma_{\text{th}}(1+k)}{(m_s-1)\bar{\gamma}}\right)^i$$
$$\leq \sum_{i=0}^\infty \left(\frac{k}{m_d+k}\right)^i \frac{(m_d)_i\,(i+1)_{m_s}}{\Gamma(i+2)\Gamma(m_s)} \left(\frac{\gamma_{\text{th}}(1+k)}{(m_s-1)\bar{\gamma}}\right)^i. \quad (21)$$

When $(m_s-1)\bar{\gamma}(m_d+k) > \gamma_{\text{th}}k(1+k)$, simplifying (20) using Pochhammer symbol identities and [14, 07.23.02.0001.01], we obtain (17).

REFERENCES

[1] M. S. Alouini and M. K. Simon, "Dual diversity over correlated log-normal fading channels," *IEEE Trans. on Commun.*, vol. 50, no. 12, pp. 1946–1959, Dec 2002.
[2] M. Yacoub, "The κ-μ distribution and the η-μ distribution," *IEEE Antennas Propag. Mag.*, vol. 49, no. 1, pp. 68–81, Feb. 2007.
[3] P. M. Shankar, "Error rates in generalized shadowed fading channels," *Wireless personal communications*, vol. 28, no. 3, pp. 233–238, 2004.
[4] P. C. Sofotasios and S. Freear, "The κ-μ/gamma composite fading model," in *IEEE Int. Conf. on Wireless Inf. Technol. and Syst.*, Honolulu, USA, Aug 2010, pp. 1–4.
[5] ——, "The η- μ/gamma composite fading model," in *IEEE International Conference on Wireless Inf. Technol. and Syst.*, Honolulu, USA, Aug 2010, pp. 1–4.
[6] S. K. Yoo, N. Bhargav, S. L. Cotton, P. C. Sofotasios, M. Matthaiou, M. Valkama, and G. K. Karagiannidis, "The κ-μ / inverse gamma and η-μ / inverse gamma composite fading models: Fundamental statistics and empirical validation," *IEEE Trans. on Commun.*, vol. PP, pp. 1–1, May 2017, DOI: 10.1109/TCOMM.2017.2780110.
[7] A. Abdi, W. C. Lau, M.-S. Alouini, and M. Kaveh, "A new simple model for land mobile satellite channels: first-and second-order statistics," *IEEE Trans. on Wireless Commun.*, vol. 2, no. 3, pp. 519–528, 2003.
[8] J. F. Paris, "Closed-form expressions for Rician shadowed cumulative distribution function," *Electron. Lett.*, vol. 46, no. 13, pp. 952–953, 2010.
[9] F. Ruiz-Vega, M. C. Clemente, P. Otero, and J. F. Paris, "Ricean shadowed statistical characterization of shallow water acoustic channels for wireless communications," *arXiv preprint arXiv:1112.4410*, 2011.
[10] I. S. Gradshteyn and I. M. Ryzhik, *Table of Integrals, Series, and Products*, 7th ed. New York: Academic, 2007.
[11] S. K. Yoo, S. L. Cotton, P. C. Sofotasios, M. Matthaiou, M. Valkama, and G. K. Karagiannidis, "The Fisher-Snedecor $\mathcal{F}$ distribution: A simple and accurate composite fading model," *IEEE Commun. Lett.*, vol. 21, no. 7, pp. 1661–1664, July 2017.
[12] Wolfram Research, Inc., *Listing of Mathematical Notations*, 2017, visited on 31/08/18. [Online]. Available: http://functions.wolfram.com/Notations/5
[13] P. Humbert, "Sur les fonctions hypercylindriques," *Comptes rendus hebdomadaires des sances de l'Acadmie des sciences (in French)*, vol. 171, pp. 490–492, 1920.
[14] Wolfram Research, Inc., 2016, visited on 03/02/17. [Online]. Available: http://functions.wolfram.com/id